LETTERS
https://doi.org/10.1038/s41558-018-0346-z

nature climate change

Contrasting responses of autumn-leaf senescence to daytime and night-time warming

Chaoyang Wu[1,2*], Xiaoyue Wang[1,2], Huanjiong Wang[1,2*], Philippe Ciais[3], Josep Peñuelas[4,5], Ranga B. Myneni[6], Ankur R. Desai[7], Christopher M. Gough[8], Alemu Gonsamo[9], Andrew T. Black[1], Rachhpal S. Jassal[10], Weimin Ju[11], Wenping Yuan[12], Yongshuo Fu[13], Miaogen Shen[14], Shihua Li[15], Ronggao Liu[16], Jing M. Chen[9] and Quansheng Ge[1,2*]

Plant phenology is a sensitive indicator of climate change[1–4] and plays an important role in regulating carbon uptake by plants[5–7]. Previous studies have focused on spring leaf-out by daytime temperature and the onset of snow-melt time[8,9], but the drivers controlling leaf senescence date (LSD) in autumn remain largely unknown[10–12]. Using long-term ground phenological records (14,536 time series since the 1900s) and satellite greenness observations dating back to the 1980s, we show that rising pre-season maximum daytime (T_{day}) and minimum night-time (T_{night}) temperatures had contrasting effects on the timing of autumn LSD in the Northern Hemisphere (> 20° N). If higher T_{day} leads to an earlier or later LSD, an increase in T_{night} systematically drives LSD to occur oppositely. Contrasting impacts of daytime and night-time warming on drought stress may be the underlying mechanism. Our LSD model considering these opposite effects improved autumn phenology modelling and predicted an overall earlier autumn LSD by the end of this century compared with traditional projections. These results challenge the notion of prolonged growth under higher autumn temperatures, suggesting instead that leaf senescence in the Northern Hemisphere will begin earlier than currently expected, causing a positive climate feedback.

Climate change over the past several decades has modified the dates of plant flowering, leaf emergence, growth stages and senescence, collectively termed phenology[13], with substantial ecological and environmental consequences[4]. Both observations and model simulations have found that air temperature has a positive influence on the onset of plant growth in the Northern Hemisphere; for example, higher spring temperature triggers earlier leaf-out and flowering dates and hence extends the growing season[8,14,15]. In contrast to those extensive research efforts on spring phenology, autumn phenology, particularly LSD, is more challenging to understand and has not received sufficient attention[16,17], while also serving as an important indicator of changing foliar physiological properties. However, autumn phenology may be as important as spring in regulating the interannual variability of carbon balance[7].

LSD has been occurring later in most regions over the past few decades[18], but providing an explanation for this change is difficult[9]. An increase in global temperature is assumed to be a driver of LSD trends[19], but studies have indicated that the contribution of temperature to LSD variability is low, especially compared with spring phenology[20,21]. We argue that ignoring the asymmetric effects[22] of T_{day} versus T_{night} and their differing impacts on LSD contributes to the reported overall low contribution of temperature to LSD variability. To test this, we used measured and gridded pre-season (defined as months from June to LSD) T_{day} and T_{night} values in the Northern Hemisphere, together with LSD data from three different datasets: (1) long-term phenological observations at ground sites from 14,536 time series since the 1900s (Supplementary Fig. 1), (2) the latest third generation of the normalized difference vegetation index (NDVI; Global Inventory Modeling and Mapping Studies NDVI3g version 1) for 1982–2015 and (3) NDVI and enhanced vegetation index (EVI) values from the Moderate-Resolution Imaging Spectroradiometer (MODIS) products for 2001–2015.

Pre-season forcing had a better predictive strength on LSD than either summer or autumn climate forcing alone (Supplementary Fig. 2). Because pre-season T_{day} and T_{night} were highly correlated, we used a partial correlation to remove the effects of T_{night} and of precipitation and radiation (similarly for T_{night}) to investigate the response of LSD to T_{day}. Correlations were classified into four types, $T_{day}^{+}T_{night}^{+}$ (typeA), $T_{day}^{-}T_{night}^{-}$ (typeB), $T_{day}^{+}T_{night}^{-}$ (typeC) and $T_{day}^{-}T_{night}^{+}$ (typeD), where T^{+} and T^{-} represent the positive and negative partial correlation coefficient, R, respectively, of temperature T with LSD.

Overall, all three datasets suggest that the onset of autumn LSD responded oppositely to T_{day} and T_{night}. The proportions of ground sites of types A and B were significantly lower than those of types C and D (Fig. 1a). More significant R values for both T_{day} and T_{night} were found within types C and D, with only two and one records out of 2,231 time series having significant R values within types

[1]The Key Laboratory of Land Surface Pattern and Simulation, Institute of Geographical Sciences and Natural Resources Research, Chinese Academy of Sciences, Beijing, China. [2]University of the Chinese Academy of Sciences, Beijing, China. [3]Laboratoire des Sciences du Climat et de l'Environnement, IPSL-LSCE CEA CNRS UVSQ, Gif-sur-Yvette, France. [4]CSIC, Global Ecology Unit CREAF-CSIC-UAB, Barcelona, Spain. [5]CREAF, Barcelona, Spain. [6]Department of Earth and Environment, Boston University, Boston, MA, USA. [7]Department of Atmospheric and Oceanic Sciences, University of Wisconsin–Madison, Madison, WI, USA. [8]Department of Biology, Virginia Commonwealth University, Richmond, VA, USA. [9]Department of Geography and Planning, University of Toronto, Toronto, Ontario, Canada. [10]Faculty of Land and Food Systems, University of British Columbia, Vancouver, British Columbia, Canada. [11]International Institute for Earth System Science, Nanjing University, Nanjing, China. [12]School of Atmospheric Sciences, Center for Monsoon and Environment Research, Sun Yat-Sen University, Guangzhou, China. [13]College of Water Sciences, Beijing Normal University, Beijing, China. [14]CAS Center for Excellence in Tibetan Plateau Earth Sciences, Beijing, China. [15]School of Resources and Environment, University of Electronic Science and Technology of China, Chengdu, China. [16]State Key Laboratory of Resources and Environmental Information System, Institute of Geographic Sciences and Natural Resources Research, CAS, Beijing, China. *e-mail: wucy@igsnrr.ac.cn; wanghj@igsnrr.ac.cn; geqs@igsnrr.ac.cn

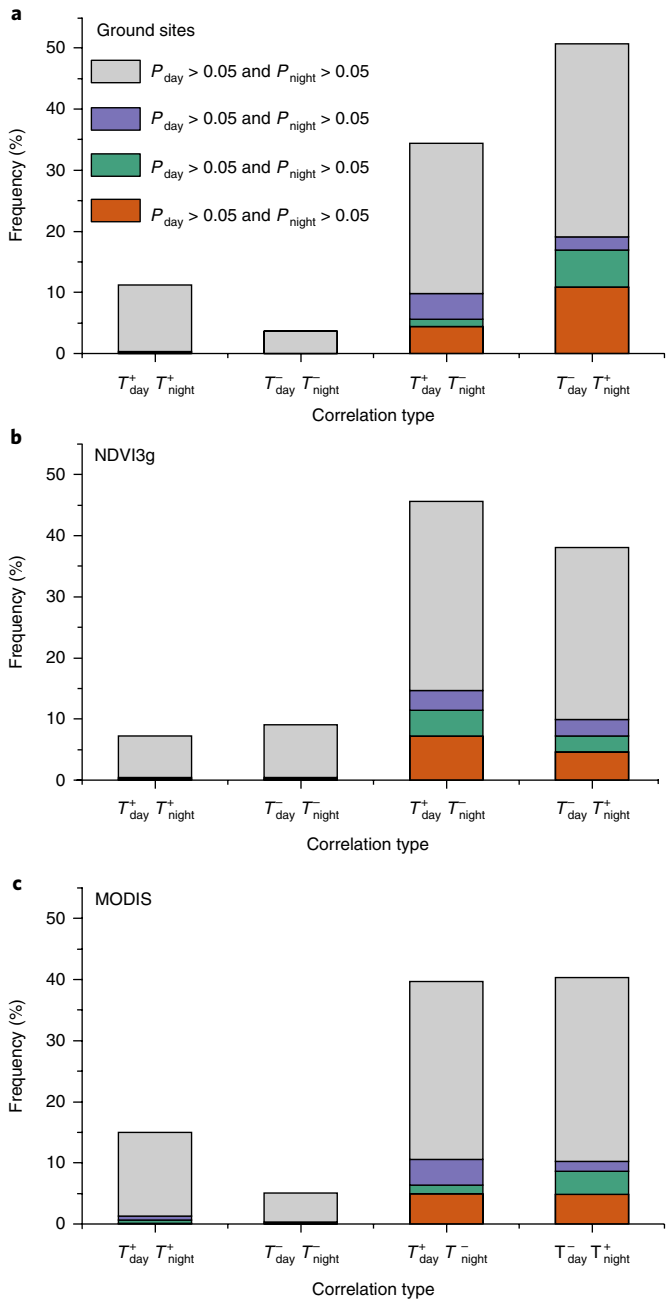

Fig. 1 | Frequency of the partial correlation coefficient between LSD and T_{day} and T_{night}. **a**, Data for 14,536 time series of ground sites. **b**, The NDVI3g dataset for 1982–2015. **c**, The MODIS product for 2001–2015. Significance was set at $P < 0.05$. The legend in **a** applies to all panels.

A and B, respectively. These results from ground sites are consistent with those for the two satellite greenness products (Fig. 1b,c). Types C and D together accounted for 83.7% and 80.0% for NDVI3g and MODIS pixels, respectively. Only 0.8% and 1.5% of the pixels had the same sign of response of LSD to T_{day} or T_{night} (that is, significant pixels for types A + B) for the NDVI3g and MODIS datasets, respectively. The NDVI3g dataset contained different fractions of types C and D (45.6% versus 38.1%), but the compositions of types C and D in NDVI3g (that is, contrasting effects of night and day temperatures) became more consistent with the MODIS results when the overlapping periods between the two sensors were considered (Supplementary Figs. 3 and 4). More details on the fractions of the four correlation types for different vegetation types are provided in Supplementary Figs. 5 and 6.

The satellite greenness products also allowed us to evaluate spatial patterns of LSD changes in response to variations in T_{day} and T_{night} (Fig. 2). For the NDVI3g data, higher T_{day} was associated with a delayed LSD for 10.7% of the pixels (mostly boreal regions) and with an earlier LSD for 7.5% of the pixels (central North America, borders of Eurasia and central China). T_{night} had evident opposite influences on LSD than T_{day}. The patterns of opposite effects from T_{day} and T_{night} on LSD were highly spatially consistent in all regions where T_{day} and T_{night} were significantly correlated with LSD. Similar results were obtained with MODIS observations (Fig. 2b,d). LSD for approximately 20% of all pixels was significantly correlated with T_{day}, of which 60.1% and 39.9% were negatively and positively correlated, respectively. The area where LSD was positively correlated with T_{night} was larger (9.4%) than the area with negative correlations (6.5%).

Vegetation grouped into Köppen–Geiger zones showed contrasting patterns between the effects of T_{day} and T_{night} on LSD (Fig. 2e,f). Type D was more widely distributed, while type C was more common for continental climates. Monsoon-influenced but not extremely cold regions and mild climates also had higher proportions of type C. Grouping these correlation types by vegetation type led to similar results (Fig. 2g,h). In theory, we would expect to find type C more in wet vegetation types and type D in dry types. The real world seems to show the same thing, but there could be many locations that do not neatly fall into that continuum, suggesting additional mechanisms may be at work, probably species adaptation.

Our results suggest that ecological trade-offs, particularly those driven by regional differences in water stress, may underlie the contrasting relationships between LSD and T_{day} and T_{night}. Type C was mostly found in humid regions where water is a less limiting factor for plant growth. In these cases, a higher T_{day}, in the likely absence of severe water stress, benefits photosynthesis, while elevated T_{night} increases night-time leaf respiration.

Explanations for the prevalence of type D relations in dry regions are more complicated. The standardized precipitation evapotranspiration index (SPEI)[23], an indicator of drought stress, accounted for the contrasting effects of increases in T_{day} and T_{night} on LSD for type D (Fig. 3). Partial correlation data indicate that increased T_{day} is negatively correlated with the SPEI (Fig. 3a), a stronger sensitivity to drought in dry regions that negatively affects plant growth and consequently leads to an earlier LSD. In contrast, we found that an increase in T_{night} is associated with a higher SPEI, that is, wetter conditions and, arguably, reduced water stress, which could extend the duration of photosynthesis and lead to delayed LSD (Fig. 3b). The latter mechanism is consistent with the generally positive partial correlation values between evapotranspiration and T_{night}, that is, more soil moisture being available for evapotranspiration in the late season, sustaining delayed LSD (Fig. 3f), and with studies showing that water stress accelerates leaf drop in dry ecosystems more than in humid ecosystems[24]. The responses of radiation to T_{day} and T_{night} may also be viewed as further evidence for the linkage between leaf senescence and plant water status to support the contrasting patterns (Supplementary Fig. 7), given that a higher T_{day} was associated with stronger radiation and potentially a higher chance of water stress. These findings suggest that dry regions, in which type D dominates, may be especially vulnerable to earlier onset of LSD if climate change reduces local precipitation and increases daytime evaporation with rising T_{day}.

Apart from physiological mechanisms relating to water stress, ecological processes may also contribute to these patterns. Warmer daytime versus night-time temperature may have contrasting effects on different species because species adaptations lead to intrinsic differences in their timing of leaf emergence and senescence that are optimized to maximize carbon gain and minimize water losses[25–27]. The ecosystem-scale responses of phenology reflect the scaled responses of ecological dynamics of multiple individual species gaining or losing a competitive advantage in a changing climate, or

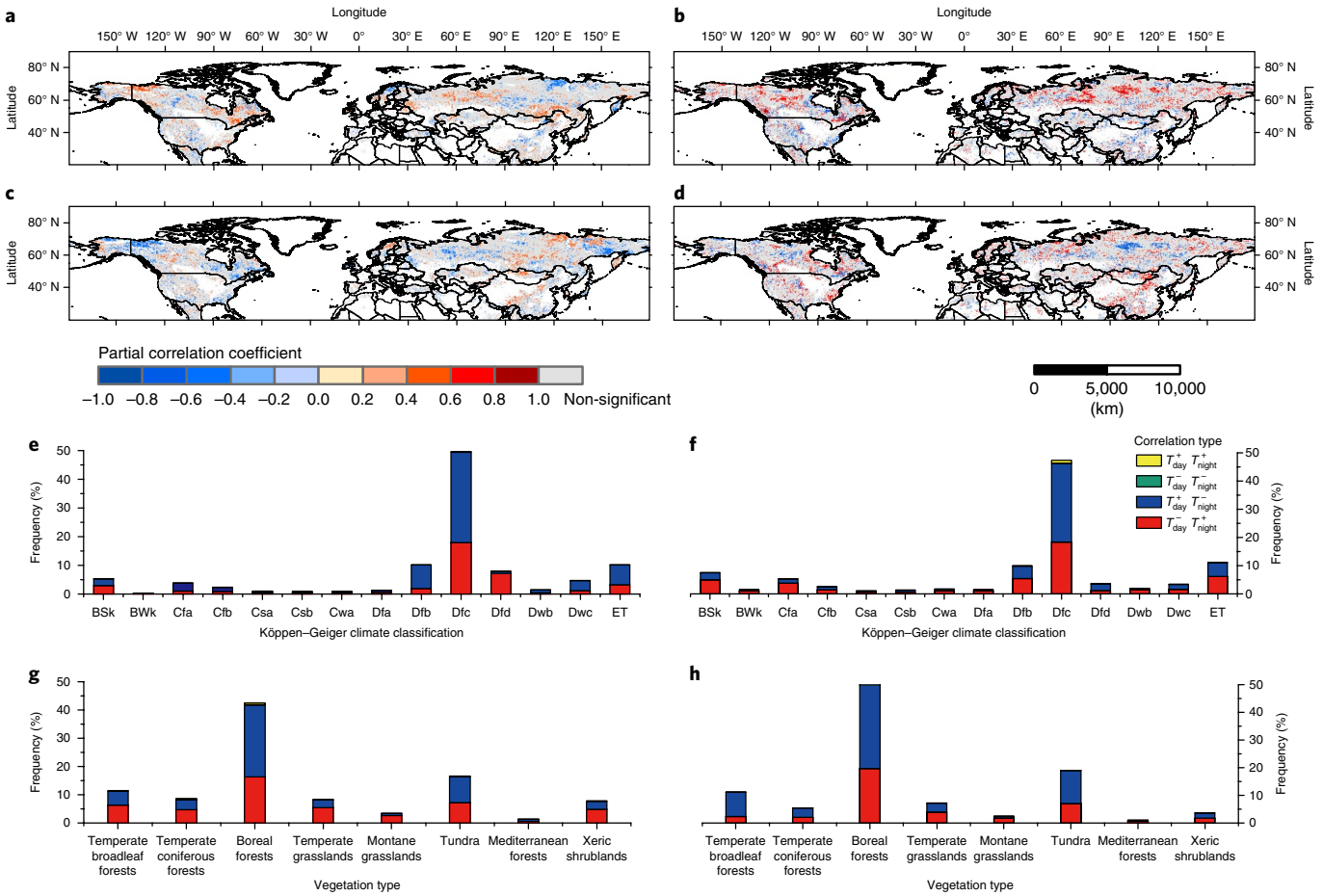

Fig. 2 | Spatial distributions of the partial correlation coefficient between LSD and T_{day} and T_{night}. **a**,**b**, LSD versus T_{day} for NDVI3g (**a**) and for the MODIS (**b**). **c**,**d**, LSD versus T_{night} for NDVI3g (**c**) and for the MODIS (**d**). **e**,**f**, Distributions of correlation types in Köppen–Geiger climate classifications using NDVI3g (**e**) and MODIS (**f**) datasets. **g**,**h**, Distributions of correlation types for vegetation types (see Methods) using NDVI3g (**g**) and MODIS (**h**) datasets. Significance was set at $P < 0.05$. The Köppen–Geiger climate classifications are detailed in Supplementary Table 2.

presenting an induced advantage as a result of land-use change and planting[17,26]. Recent results suggest that the magnitude of phenological change to effects by shifts in plant species composition may be similar to that by climate change[27], and the autumn phenology may thus change accordingly.

We tested the implications of the observation analysis on future trends in autumn LSD by developing a weighted day–night-temperature growing-degree-day (DN_{GDD}) algorithm incorporating these opposite changes in LSD to T_{day} and T_{night} (see Methods). Our model substantially improved LSD modelling (in terms of R (Supplementary Figs. 8–10), root mean square error (Supplementary Figs. 11–13) and percentage of significant pixels (Supplementary Figs. 14 and 15)) compared with currently used threshold or GDD methods, both for the overall dataset and for vegetation types.

Spatial patterns of improvements using the MODIS and NDVI3g were also investigated (Supplementary Figs. 16 and 17). The results from the MODIS and the ground sites (Supplementary Fig. 18) were more consistent with our model, and the accuracy of the threshold method was much lower, so we used the coefficients from the MODIS data to predict LSD variability by the end of this century using the DN_{GDD} and traditional GDD algorithms under two Representative Concentration Pathway (RCP) scenarios (RCP 4.5 and RCP 8.5) (Supplementary Fig. 19 and Fig. 4).

LSD from the DN_{GDD} method was overall earlier than conventional predictions across Köppen–Geiger climate classification types. Globally, LSD was earlier for about 68% of the terrestrial biosphere under RCP 4.5 and for about 70% under RCP 8.5. LSD was mostly later for central North America, western Russia and southwestern China. Most vegetation types showed earlier LSD estimates under the two RCP scenarios, while the temperate grasslands were expected to have later senescence dates.

Climatic variability, particularly temperature, has driven phenological changes over the past several decades, but has been challenging to predict. The ability to predict autumn LSD is particularly limited. We report, using 14,536 ground time series and more than 30 years of remotely sensed observations, the opposite responses of LSD to daytime and night-time warming, providing a perspective to account for the previous low estimation accuracy of autumn LSD when relying solely on mean temperature. A model based on mean temperature cannot correctly predict LSD changes, because LSD responds to T_{day} and T_{night} in opposite directions. Our results also provide a perspective to account for the carry-over effects between spring and autumn phenology, that is, the start and end of a growing season always move in the same direction[28]. An earlier start of a season is mainly triggered by higher spring temperatures, with increased growth depleting soil water[29], which is then associated with autumn drought, inducing a reduction in growth and consequently leading to an earlier end to the growing season[30].

Our improvement in modelling autumn phenology is strong and convincing evidence for the value of incorporating daytime

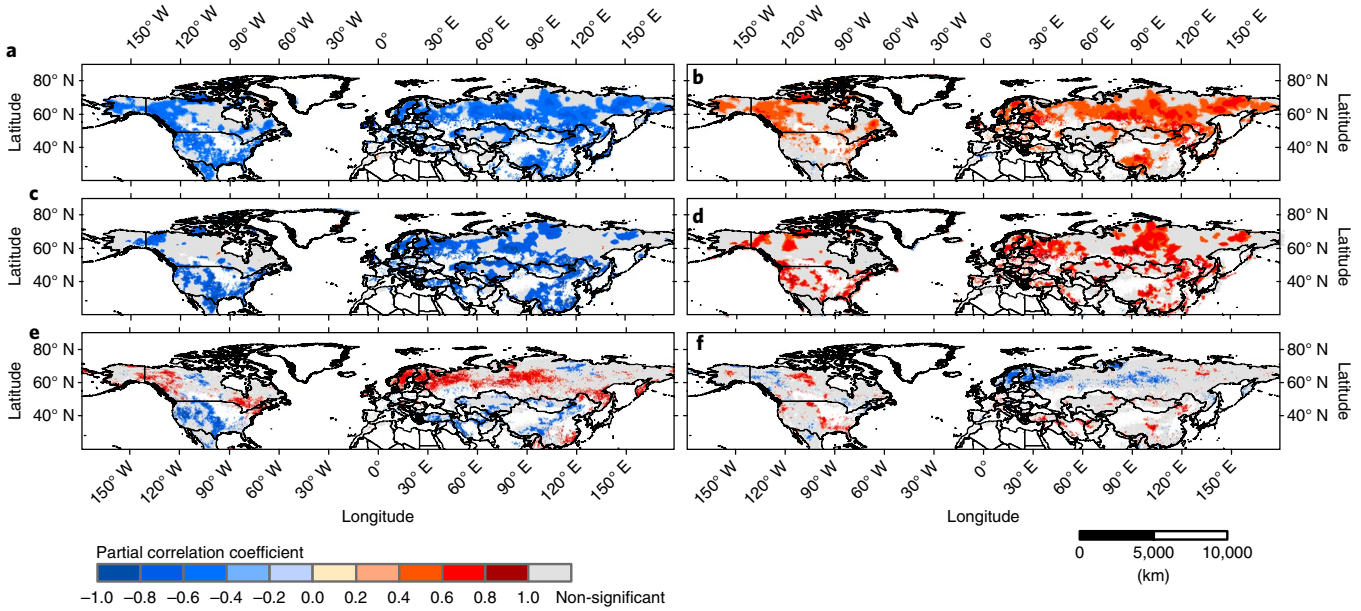

Fig. 3 | The partial correlation coefficient between the SPEI, evapotranspiration, T_{day} and T_{night}. **a**,**b**, SPEI versus T_{day} (**a**) and T_{night} (**b**) for NDVI3g. **c**,**d**, SPEI versus T_{day} (**c**) and T_{night} (**d**) for the MODIS. **e**,**f**, Evapotranspiration versus T_{day} (**e**) and T_{night} (**f**) for the MODIS. Significance was set at $P < 0.05$.

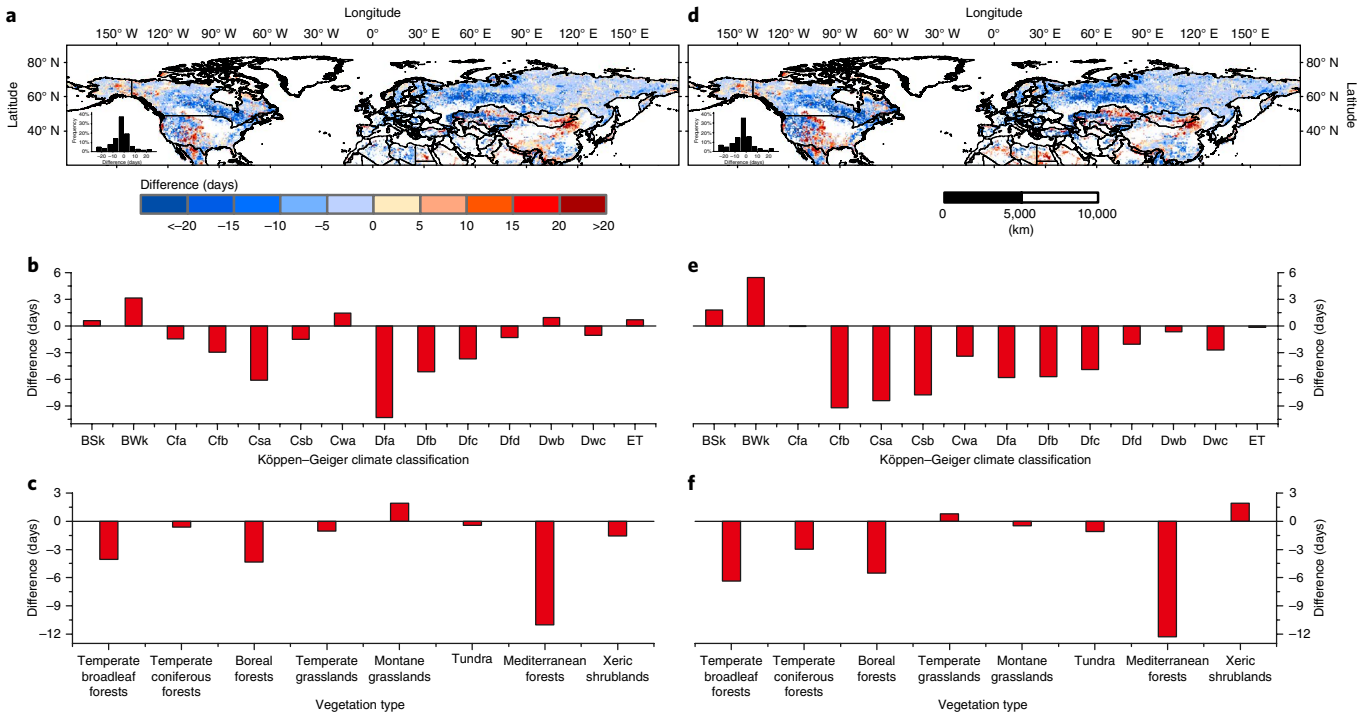

Fig. 4 | LSD differences from the weighted DN_{GDD} and traditional GDD ($LSD_{DNGDD} - LSD_{GDD}$) models under two RCP scenarios. a–c, $LSD_{DNGDD} - LSD_{GDD}$ under RCP 4.5 (**a**), with averages of differences for the Köppen-Geiger climate classification (**b**) and vegetation types (**c**). **d**–**f**, $LSD_{DNGDD} - LSD_{GDD}$ under RCP 8.5 (**d**), with averages of differences for the Köppen-Geiger climate classifications (**e**) and vegetation types (**f**). The Köppen-Geiger climate classifications are detailed in Supplementary Table 2.

and night-time temperatures in terrestrial models, rather than mean temperature alone. The application of this model projects an overall earlier than currently expected start of autumn senescence in the Northern Hemisphere by the end of this century, particularly in dry regions. The earlier data of autumn senescence may be a potentially unrecognized positive feedback to climate change and consequently a weakening in the capability of terrestrial carbon uptake.

Online content

Any methods, additional references, Nature Research reporting summaries, source data, statements of data availability and associated accession codes are available at https://doi.org/10.1038/s41558-018-0346-z.

Received: 29 December 2017; Accepted: 23 October 2018;
Published online: 26 November 2018

References

1. Fu, Y. H. et al. Declining global warming effects on the phenology of spring leaf unfolding. *Nature* **526**, 104–107 (2015).
2. Xia, J. et al. Joint control of terrestrial gross primary productivity by plant phenology and physiology. *Proc. Natl Acad. Sci. USA* **112**, 2788–2793 (2015).
3. Buitenwerf, R., Rose, L. & Higgins, S. I. Three decades of multi-dimensional change in global leaf phenology. *Nat. Clim. Change* **5**, 364–368 (2015).
4. Peñuelas, J., Rutishauser, T. & Filella, I. Phenology feedbacks on climate change. *Science* **324**, 887–888 (2009).
5. Richardson, A. D. et al. Climate change, phenology, and phenological control of vegetation feedbacks to the climate system. *Agr. Forest Meteorol.* **169**, 156–173 (2013).
6. Keenan, T. F. et al. Net carbon uptake has increased through warming-induced changes in temperate forest phenology. *Nat. Clim. Change* **4**, 598–604 (2014).
7. Wu, C. et al. Interannual variability of net ecosystem productivity in forests is explained by carbon flux phenology in autumn. *Glob. Ecol. Biogeogr.* **22**, 994–1006 (2013).
8. Piao, S. et al. Leaf onset in the Northern Hemisphere triggered by daytime temperature. *Nat. Commun.* **6**, 6911 (2015).
9. Pulliainen, J. et al. Early snowmelt significantly enhances boreal springtime carbon uptake. *Proc. Natl Acad. Sci. USA* **114**, 11081–11086 (2017).
10. Liu, Q. et al. Delayed autumn phenology in the Northern Hemisphere is related to change in both climate and spring phenology. *Glob. Change Biol.* **22**, 3702–3711 (2016).
11. Keenan, T. F. & Richardson, A. D. The timing of autumn senescence is affected by the timing of spring phenology: implications for predictive models. *Glob. Change Biol.* **21**, 2634–2641 (2015).
12. Gill, A. L. et al. Changes in autumn senescence in Northern Hemisphere deciduous trees: a meta-analysis of autumn phenology studies. *Ann. Bot.* **116**, 875–888 (2015).
13. Myneni, R. B., Keeling, C. D., Tucker, C. J., Asrar, G. & Nemani, R. R. Increased plant growth in the northern high latitudes from 1981 to 1991. *Nature* **386**, 698–702 (1997).
14. Suni, T. et al. Air temperature triggers the recovery of evergreen boreal forest photosynthesis in spring. *Glob. Change Biol.* **9**, 1410–1426 (2003).
15. Richardson, A. D. et al. Terrestrial biosphere models need better representation of vegetation phenology: results from the North American carbon program site synthesis. *Glob. Change Biol.* **18**, 566–584 (2012).
16. Gallinat, A. S., Primack, R. B. & Wagner, D. L. Autumn, the neglected season in climate change research. *Trends Ecol. Evol.* **30**, 169–176 (2015).
17. Walther, G. R. et al. Ecological responses to recent climate change. *Nature* **416**, 389–395 (2002).
18. Zhu, W. et al. Extension of the growing season due to delayed autumn over mid and high latitudes in North America during 1982–2006. *Glob. Ecol. Biogeogr.* **21**, 260–271 (2012).
19. Garonna, I. et al. Strong contribution of autumn phenology to changes in satellite-derived growing season length estimates across Europe (1982–2011). *Glob. Change Biol.* **20**, 3457–3470 (2014).
20. Yang, Y., Guan, H., Shen, M., Liang, W. & Jiang, L. Changes in autumn vegetation dormancy onset date and the climate controls across temperate ecosystems in China from 1982 to 2010. *Glob. Change Biol.* **21**, 652–665 (2015).
21. Jeong, S. J., Ho, C. H., Gim, H. J. & Brown, M. E. Phenology shifts at start vs. end of growing season in temperate vegetation over the Northern Hemisphere for the period 1982–2008. *Glob. Change Biol.* **17**, 2385–2399 (2011).
22. Peng, S. et al. Asymmetric effects of daytime and night-time warming on Northern Hemisphere vegetation. *Nature* **501**, 88–92 (2013).
23. Beguería, S., Vicente-Serrano, S. M., Reig, F. & Latorre, B. Standardized precipitation evapotranspiration index (SPEI) revisited: parameter fitting, evapotranspiration models, tools, datasets and drought monitoring. *Int. J. Climatol.* **34**, 3001–3023 (2014).
24. Meng, T. T., Ni, J. & Harrison, S. P. Plant morphometric traits and climate gradients in northern China: a meta-analysis using quadrat and flora data. *Ann. Bot.* **104**, 1217–1229 (2009).
25. Prasad, V. K., Badarinath, K. V. S. & Eaturu, A. Spatial patterns of vegetation phenology metrics and related climatic controls of eight contrasting forest types in India—analysis from remote sensing datasets. *Theor. Appl. Climatol.* **89**, 95–107 (2007).
26. Peñuelas, J. et al. Evidence of current impact of climate change on life: a walk from genes to the biosphere. *Glob. Change Biol.* **19**, 2303–2338 (2013).
27. Wolf, A. A., Zavaleta, E. S. & Selmants, P. C. Flowering phenology shifts in response to biodiversity loss. *Proc. Natl Acad. Sci. USA* **114**, 3463–3468 (2017).
28. Fu, Y. S. et al. Variation in leaf flushing date influences autumnal senescence and next year's flushing date in two temperate tree species. *Proc. Natl Acad. Sci. USA* **111**, 7355–7360 (2014).
29. Wolf, S. et al. Warm spring reduced carbon cycle impact of the 2012 US summer drought. *Proc. Natl Acad. Sci. USA* **113**, 5880–5885 (2016).
30. Peñuelas, J. et al. Shifting from a fertilization-dominated to a warming-dominated period. *Nat. Ecol. Evol.* **1**, 1438–1445 (2017).

Acknowledgements

This work was funded by the Strategic Priority Research Program of the Chinese Academy of Sciences (XDA19040103), International Cooperation and Exchange Programs of National Science Foundation of China (Sino-German, 41761134082), National Natural Science Foundation of China (41522109) and the Key Research Program of Frontier Sciences, CAS (QYZDB-SSW-DQC011). J.P. and P.C. were funded by European Research Council Synergy grant ERC-SyG-2013-610028 IMBALANCE-P. A.R.D. acknowledges support from the Ned P. Smith Professorship of Climatology, University of Wisconsin–Madison.

Author contributions

C.W., H.W. and Q.G. designed the research. C.W. wrote the first draft of the paper. J.P. and P.C. extensively revised the writing. H.W. performed the site model simulations. X.W. performed remote-sensing model simulations. All the authors contributed to writing the paper.

Competing interests

The authors declare no competing interests.

Additional information

Supplementary information is available for this paper at https://doi.org/10.1038/s41558-018-0346-z.

Reprints and permissions information is available at www.nature.com/reprints.

Correspondence and requests for materials should be addressed to C.W. or H.W. or Q.G.

Publisher's note: Springer Nature remains neutral with regard to jurisdictional claims in published maps and institutional affiliations.

Methods

Phenological observation data. We used observations of LSD from three independent phenological datasets.

(1) The Pan European Phenology Project PEP725 (ref. [31]), an open-access database with long-term plant phenological observations (since 1868) from 19,608 sites and 78 species across 25 European countries.

(2) The Chinese Phenological Observation Network, with data since 1963 for >100 species at 42 sites across China[32].

(3) LSD data for two tree species (*Acer palmatum* and *Ginkgo biloba*) at 54 meteorological stations in South Korea for 1989–2007[33].

The definitions of LSD notably differ among the datasets. LSD for the PEP725, Chinese Phenological Observation Network and South Korean datasets is defined as the date when 50%, 90% and 20% of the tree leaves, respectively, change colour from green to red or yellow. We removed outliers using methods[34] to exclude potential biases and inadequate degrees of freedom and focused on time series with at least 15 years of records for 1900–2015. We thus analysed 14,536 LSD time series for 24 species (Supplementary Table 1).

LSD derived from satellite data. LSD in the Northern Hemisphere was determined using two satellite-derived vegetation indices, the NDVI and the EVI (ref. [35]). Both the NDVI and the EVI are direct indicators of vegetation growth and have been widely applied for investigating vegetation phenology[36]. We used two datasets to reduce the uncertainties caused by a single data source: NDVI3g data derived from the Advanced Very-High-Resolution Radiometer, and NDVI and EVI values derived from the MODIS. The NDVI3g data have a spatial resolution of 1/12°, a half-month interval and a 34-year time span (1982–2015). The MODIS 16-day composite product MOD13C1 (Collection 6) includes both NDVI and EVI values with a 0.05° resolution for 2001–2015.

We eliminated the impacts of areas with sparse vegetation from the results by first excluding pixels with annual NDVI < 0.1 or annual EVI < 0.08 (ref. [37]). A Savitzky–Golay filter was then used to smooth the NDVI (EVI) time series[38]. We then estimated LSD using two methods.

The first method was a dynamic-threshold approach, which uses an annually defined threshold for each pixel based on the NDVI ratio:

$$\mathrm{NDVI}_{\mathrm{ratio}} = (\mathrm{NDVI}-\mathrm{NDVI}_{\mathrm{min}})/(\mathrm{NDVI}_{\mathrm{max}}-\mathrm{NDVI}_{\mathrm{min}}) \quad (1)$$

where NDVI is the daily NDVI, and $\mathrm{NDVI}_{\mathrm{max}}$ and $\mathrm{NDVI}_{\mathrm{min}}$ are the annual daily maximum and minimum NDVI, respectively. The $\mathrm{NDVI}_{\mathrm{ratio}}$ ranges from 0 to 1. LSD is determined when $\mathrm{NDVI}_{\mathrm{ratio}}$ decreases to 0.5 in autumn[39,40].

The second method was based on a series of piecewise logistic functions. The NDVI time series were first divided into two sections by the maximum daily NDVI in each year, and a double logistic function was applied to fit each section[41]:

$$y(t) = a_1 + (a_2 - a_7 t)\left[\frac{1}{1+e^{(a_3-t)/a_4}} - \frac{1}{1+e^{(a_5-t)/a_6}}\right] \quad (2)$$

where $y(t)$ is the NDVI at day of year t and a_1–a_7 are fitting parameters. LSD was then defined as the time when the curvature changing rate reached its last local maximum value.

For NDVI3g data, we calculated LSD using the NDVI from both the dynamic-threshold approach and the piecewise logistic function method. Since the MODIS sensor provides the EVI, we further used an EVI-based logistic function method to derive LSD. To sum up, for the NDVI3g data, average LSD from a threshold approach and logistic function method were used, and for the MODIS data, an additional LSD from an EVI-based logistic function method was used (not for MODIS NDVI data).

At high latitudes (or elevations), snow cover is important for regional climate and arrives early in autumn, potentially masking evergreen vegetation. However, we have suggested that using a Savitzky–Golay filter could solve the noise from a 'sudden' change in the time series of the NDVI due to snow[38]. In particular, a previous study showed that snowfall had little influence on determining the end of a growing season in western Arctic Russia[42]. For high elevations, our previous analysis on the Tibetan Plateau showed that for more than 98% of regions, snow occurred later than LSD[43].

Climatic data. We used the CRU-TS (Climatic Research Unit Time Series) 4.00 dataset with a spatial resolution of 0.5° × 0.5° for 1901–2015[44]. We extracted monthly data for maximum temperature, T_{max}, minimum temperature, T_{min}, mean temperature, T_{mean}, precipitation and cloud cover from this dataset for analysing LSD from in-situ observations and the two remote-sensing datasets. We modelled past and future LSD by temperature by acquiring daily gridded data for maximum and minimum temperature with a spatial resolution of 0.5° from the National Oceanic and Atmospheric Administration Earth System Research Laboratory's Physical Sciences Division for 1982–2015. We used daily T_{max} and T_{min} simulated by the CCSM (Community Climate System Model) 4.0 under two climatic scenarios (RCP 4.5 and RCP 8.5) for future climatic data (2081–2100). These data were from an open-access database of the Coupled Model Intercomparison Project Phase 5.

Analyses. We used partial correlation analyses to determine the responses of LSD to T_{day} and T_{night}. The reason was that directly correlating LSD to T_{day} would give misleading results because T_{night} is a confounding variable that is numerically related to both LSD and T_{day}, violating independence of variables in multiple correlation tests. Thus, using the partial correlation between LSD and T_{day} would measure the degree of association with the effect of a set of controlling random variables removed (for example, T_{night}, precipitation, radiation), given that these factors have shown strong influences on LSD[10,20]. Since a previous study demonstrated that clouds are the main atmospheric factor modulating the surface incidence of solar radiation[45], cloud cover data were used to model the effect of radiation on LSD, as similarly conducted in previous analyses[8]. An R value of at least 0.514 for the MODIS is required for the significance test (P=0.05), but this value decreases to 0.339 for the longer NDVI3g data. These analyses were investigated for both Köppen–Geiger climate classifications and vegetation types (Supplementary Table 2)[46,47]. Crops were excluded because their signal may result from changes in cropping or harvest cycles, rather than from climate change. Furthermore, since, at low latitudes, plant phenology of tropical and subtropical areas responds to factors other than temperature, regions with latitudes of <20° N were also excluded.

Current phenology algorithms in most terrestrial-biosphere models are based solely on temperatures in the preceding months[15,48]. We determined the length of the pre-season whose average T_{day} had the most influence on LSD, by calculating the partial correlation coefficients between LSD and mean T_{day} during 0, 1, 2, … n months before LSD, controlling for corresponding mean T_{night}, total precipitation and radiation. The maximum range (n) of the pre-season is generally from June to the multiyear mean date of LSD (see, for example, Supplementary Fig. 20). The partial correlation coefficients with the highest absolute values were then used in the following analysis. We obtained the relationship between LSD and T_{night} in the same way, but replacing T_{day} with T_{night}. This analytical procedure was applied for observed LSD from ground sites and derived LSD from the MODIS and NDVI3g data.

Models for predicting LSD. Our results indicated that LSD responded oppositely to T_{day} and T_{night}, so we developed a weighted $\mathrm{DN}_{\mathrm{GDD}}$ algorithm from observations to model LSD, and compared the algorithm with currently used threshold and GDD models based on T_{mean} (ref. [49]).

The threshold model was the simplest method. We calculated average T_{mean} for five days before LSD in each year and used the multiyear mean value as the threshold to model LSD. If T_{mean} was lower than the threshold for five consecutive days from 1 July, the last date was considered the LSD.

GDD was calculated as

$$\mathrm{GDD}(d) = \max(T_{\mathrm{b}} - T_{\mathrm{mean}}(d), 0) \quad (3)$$

$$\mathrm{GDD}_{\mathrm{threshold}} = \sum_{d=d_0}^{\mathrm{LSD}} \mathrm{GDD}(d) \quad (4)$$

where $\mathrm{GDD}(d)$ is the acquired growing degree at a date d, $\mathrm{GDD}_{\mathrm{threshold}}$ is the requirement of accumulated growing degree from d_0 to LSD, T_{b} is the base temperature set to 15 °C, 20 °C, 25 °C and 30 °C, $T_{\mathrm{mean}}(d)$ is the mean daily temperature and d_0 is the date on which the calculation begins (1 July in this study). LSD is the observed or derived date of leaf colouring in each year. The date when $\mathrm{GDD}(d)$ exceeded the multiyear average GDD threshold was defined as the LSD.

Our $\mathrm{DN}_{\mathrm{GDD}}$ model improved on the original GDD model and was calculated by

$$\mathrm{GDD}(d) = k \times \max(T_{\mathrm{b}} - T_{\mathrm{day}}(d), 0) + (1-k) \times \max(T_{\mathrm{b}} - T_{\mathrm{night}}(d), 0) \quad (5)$$

where $T_{\mathrm{day}}(d)$ is the daily maximum temperature, $T_{\mathrm{night}}(d)$ is the daily minimum temperature and k is the weighting factor. When $0 < k < 1$, the effects of T_{day} and T_{night} on LSD are consistently positive; when $k > 1$ or $k < 0$, the effects of T_{day} and T_{night} on LSD are opposite. To determine the value of k, we first calculated the ratio of R_{day} to R_{night} for each station or pixel, and found that 99.9% of the ratio values were between −10 and 10 for both ground and satellite data (Supplementary Fig. 21). In other words, the level of T_{day} (T_{night}) effect could be 1 to 10 times the level of T_{night} (T_{day}) effect (note that T_{day} represents T_{day} with the effects of T_{night} removed). Therefore, the values of k ranged from −1 to 2 (see Supplementary Table 3). In addition, when k tends to infinity, the effects of T_{day} and T_{night} on LSD are opposite, with the same level.

We evaluated the accuracy and obtained the most appropriate parameters of the models by calculating R and the root mean square error between modelled and observed LSD. T_{b} and k with the lowest root mean square error were considered to be the most appropriate values for each site or pixel.

Code availability. All code used for data processing in this study is available from the corresponding author upon request.

Data availability

The data that support the findings of this study are available from the corresponding author upon request.

References

31. Templ, B. et al. Pan European Phenological database (PEP725): a single point of access for European data. *Int. J. Biometeorol.* **62**, 1109–1113 (2018).
32. Ge, Q., Wang, H., Rutishauser, T. & Dai, J. Phenological response to climate change in China: a meta-analysis. *Glob. Change Biol.* **21**, 265–274 (2015).
33. Park, C. K., Ho, C.-H., Jeong, S.-J., Lee, E. J. & Kim, J. Spatial and temporal changes in leaf coloring date of *Acer palmatum* and *Ginkgo biloba* in response to temperature increases in South Korea. *PLoS ONE* **12**, e0174390 (2017).
34. Schaber, J. & Badeck, F. W. Evaluation of methods for the combination of phenological time series and outlier detection. *Tree Physiol.* **22**, 973–982 (2002).
35. Huete, A. et al. Overview of the radiometric and biophysical performance of the MODIS vegetation indices. *Remote Sens. Environ.* **83**, 195–213 (2002).
36. Zhang, X. et al. Monitoring vegetation phenology using MODIS. *Remote Sens. Environ.* **84**, 471–475 (2003).
37. Shen, M. et al. Increasing altitudinal gradient of spring vegetation phenology during the last decade on the Qinghai–Tibetan Plateau. *Agr. Forest Meteorol.* **189**, 71–80 (2014).
38. Chen, J. et al. A simple method for reconstructing a high-quality NDVI time-series data set based on the Savitzky–Golay filter. *Remote Sens. Environ.* **91**, 332–344 (2004).
39. Piao, S. et al. Changes in satellite-derived vegetation growth trend in temperate and boreal Eurasia from 1982 to 2006. *Glob. Change Biol.* **17**, 3228–3239 (2011).
40. White, M. A., Thornton, P. E. & Running, S. W. A continental phenology model for monitoring vegetation responses to interannual climatic variability. *Glob. Biogeochem. Cycles* **11**, 217–234 (1997).
41. Elmore, A. J., Guinn, S. M., Minsley, B. J. & Richardson, A. D. Landscape controls on the timing of spring, autumn, and growing season length in mid-Atlantic forests. *Glob. Change Biol.* **18**, 656–674 (2012).
42. Zeng, H. & Jia, G. Impacts of snow cover on vegetation phenology in the Arctic from satellite data. *Adv. Atmos. Sci.* **30**, 1421–1432 (2013).
43. Wang, X., Wu, C., Peng, D., Gonsamo, A. & Liu, Z. Snow cover phenology affects alpine vegetation growth dynamics on the Tibetan Plateau: satellite observed evidence, impacts of biomes, and climate drivers. *Agr. Forest Meteorol.* **256**, 61–74 (2018).
44. Harris, I., Jones, P. D., Osborn, T. J. & Lister, D. H. Updated high-resolution grids of monthly climatic observations—the CRU TS3.10 Dataset. *Int. J. Climatol.* **34**, 623–642 (2014).
45. Silva, A. A. & de Souza Echer, M. P. Ground-based measurements of local cloud cover. *Meteorol. Atmos. Phys.* **120**, 201–212 (2013).
46. Olson, D. M. et al. Terrestrial ecoregions of the world: a new map of life on Earth. *Bioscience* **51**, 933–938 (2001).
47. Peel, M. C., Finlayson, B. L. & McMahon, T. A. Updated world map of the Köppen-Geiger climate classification. *Hydrol. Earth Syst. Sci.* **11**, 1633–1644 (2007).
48. Delpierre, N. et al. Modelling interannual and spatial variability of leaf senescence for three deciduous tree species in France. *Agr. Forest Meteorol.* **149**, 938–948 (2009).
49. Krinner, G. et al. A dynamic global vegetation model for studies of the coupled atmosphere-biosphere system. *Glob. Biogeochem. Cycles* **19**, GB1015 (2005).